# CHAPTER 4

# A CHIRAL DECORATED METAL–NICOTINATE FRAMEWORK

In recent years, the study of chiral MOMs has received much attention owning to their potential applications in catalysis, chiral separation, pharmaceutical and biomedical industries [1–4]. Several approaches have been previously reported for the predictable creation of chiral, polymeric, coordination frameworks [5–11]. In particular, these MOMs can be formed from chiral ligands or by using auxiliary ligands that decorate the framework. In some cases these auxiliary ligands have been shown to direct the chirality of the helices present in the structure [12].

Amino acids are good candidates as chiral building blocks, especially as low–cost naturally occurring examples. They are interesting biological ligands which can bind to metal ions using multiple functional groups including carboxylate and/or amino parts [13]. From a structural point of view, *L*–tyrosine is considered as one of the most interesting amino acid ligands, which can chelate to metal ions through the $\alpha$–amino acid and also bond through the hydroxyl group attached to the aromatic ring [14, 15]. The synthesis based on using a mixed–ligand approach is still a challenge in the construction of new MOMs because of the difficulty in predicting the outcome of coordination, but it potentially offers facile tuning of structural, topological and functional features derived from different components. Ligands derived from carboxylates are the subject of extensive research because they have versatile coordination modes [16]. These can coordinate to a transition metal or lanthanide ion in flexible modes including a monodentate, bidentate chelating or bridging fashion depending on several variables within the system, such as coordination preference of the metal and metal size, and the nature of the solvent present. The predictable chemistry of carboxylic acids in the presence of other ligands such as pyridine is one of their most desirable features. Recipes employing carboxylate ligands are now well established [17, 18].

Here, the microwave–assisted hydrothermal synthesis was employed in growing crystals of two new 1–D MOMs; $Co(C_9H_{10}NO_3)(C_6H_4NO_2)(H_2O)_2$ (**II**) and $Ni(C_9H_{10}NO_3)(C_6H_4NO_2)(H_2O)_2$ (**III**), which are isostructural and contain tyrosine functioning as ligand and the isonicotinic acid as bidentate linker.

## 4.1 Experimental

### 4.1.1 Microwave–assisted hydrothermal crystal growth and initial characterization

Crystals **II** and **III** were readily synthesized under the same conditions using the microwave–assisted hydrothermal technique. In order to prepare the ligand solution, 1.0 mol·dm$^{-3}$ $NaOH_{(aq)}$ was slowly dropped into a mixture of *L*–4–hydroxyphenylalanine (*L*–tyrosine; 0.0924 g, 0.5 mmol; Sigma Aldrich, 98%,) and 4–pyridinecarboxylic acid (isonicotinic acid; 0.0616 g, 0.5 mmol; Sigma Aldrich, 99%) in deionized water (10.0 cm$^3$) until complete dissolution was achieved. 5.0 mL of an aqueous solution of $Co(CH_3COO_2)_2·4H_2O$ (0.2491, 1.0 mmol; Fisher Chemical) or $Ni(CH_3COO_2)_2·4H_2O$ (0.2539 g, 1.0 mmol; Alfa Aesar, 98%) was then added to the above solution and subsequently adjusting the final pH value to 8 by the addition of 1.0 mol·dm$^{-3}$ $NaOH_{(aq)}$. The reaction mixtures were stirred at 70 °C for 30 min before being transferred into a sealed 31.0 cm$^3$ Teflon vessel and then placed in a water bath (microwavable plastic bowl) that contained *ca.*1.5 dm$^3$ water at 95(±5) °C. The whole set of the apparatus was located in a domestic microwave oven (Prestige, Model: SM23, 800 W, 2.45 GHz) using a constant power of approximately 616 W for 2 hours. The reactions were kept in a water bath overnight in order to achieve cooling to room temperature.

The FT–IR spectra were collected on the ground crystals prepared as KBr disks (1:20 dilution) using a Perkin Elmer FT–IR Spectrometer Spectrum RX1 between 4000–400 cm$^{-1}$. In order to study the thermal stability, the crystals were loaded into alumina pans and were heated in the temperature range of 50–700 °C with a heating rate of 10 °C·min$^{-1}$ under a nitrogen atmosphere using a Mettler Toledo TGA/DSC 1.

Chemical analysis for $C_{15}H_{18}N_2CoO_7$ (**II**); Anal. Calc. (%): C, 45.31; H, 4.53; N, 7.05. Found (%): C, 45.09; H, 4.44; N, 6.90. For $C_{15}H_{18}N_2NiO_7$ (**III**); Anal. Calc. (%): C, 45.34; H, 4.53; N, 7.05. Found (%): C, 45.19; H, 4.37; N, 6.94.

### 4.1.2 Structure determination and refinement

The X–ray diffraction data were collected on a Stoe IPDS2 diffractometer with graphite monochromator using Mo *Kα* radiation (λ = 0.71073 Å) at 290 *K* in a series of *ω*–scans. The collections were conducted on an orange–pink block crystal (0.22 × 0.20 × 0.15 mm$^3$) and a blue plate crystal (0.15 × 0.14 × 0.10 mm$^3$) for **II** and **III**, respectively. Structures were refined using full–matrix least squares refinement employing all unique data within SHELXL–97 [19]. The crystallographic details and refinement parameters for **II** and **III** are given in Table 4.1. The refined atomic coordinates and equivalent isotropic displacement parameters for the data of **II** and **III** are provided in Tables 4.2 and 4.3. Tables 4.4–4.5 list selected bond distances about the metal centers for the reported compounds.

**Table 4.1** Crystal and experimental data for **II** and **III**.

| **Identification code** | **II** | **III** |
|---|---|---|
| Molecular formula | $Co(C_9H_{10}NO_3)(C_6H_4NO_2)(H_2O)_2$ | $Ni(C_9H_{10}NO_3)(C_6H_4NO_2)(H_2O)_2$ |
| Empirical formula | $C_{15}H_{18}N_2O_7Co$ | $C_{15}H_{18}N_2O_7Ni$ |
| Formula weight | 397.24 | 397.02 |
| Crystal size (mm$^3$) | 0.22 × 0.20 × 0.15 | 0.15 × 0.14 × 0.10 |
| Crystal system | Monoclinic | Monoclinic |
| Space group | $P2_1$ | $P2_1$ |
| $a$ (Å) | 6.0658(6) | 6.0946(8) |
| $b$ (Å) | 15.540(2) | 15.443(2) |
| $c$ (Å) | 9.1328(9) | 9.1202(11) |
| $\beta$ (°) | 107.052(7) | 107.803(10) |
| $V$ (Å$^3$) | 823.05(16) | 817.28(19) |
| $Z$ | 2 | 2 |
| $T$ $(K)$ | 290(2) | 290(2) |
| $\rho_{\text{calc.}}$ (g·cm$^{-3}$) | 1.603 | 1.613 |
| $\lambda$ (Mo Kα) (Å) | 0.71073 | 0.71073 |
| $\mu$ (mm$^{-1}$) | 1.084 | 1.229 |
| $\theta$ range (°) | 2.62–29.21 | 2.35–25.51 |
| Unique data | 7315 | 4720 |
| Observed data | 4291 | 3021 |
| Parameters no. | 240 | 239 |
| Restrains no. | 7 | 25 |
| Goodness of fit | 0.893 | 0.891 |
| $R$, $R_w$ (all data) | 0.0468, 0.0795 | 0.1009, 0.1992 |
| $R$, $R_w$ (I/2σ(I)) | 0.0321, 0.0730 | 0.0702, 0.1842 |

**Table 4.2** Atomic coordinates and equivalent isotropic displacement parameters for **II**.

| | ***x*** | ***y*** | ***z*** | ***Ueq*** **(Å$^2$)** |
|---|---|---|---|---|
| Co1 | -0.21365(5) | 0.12087(2) | 0.07315(4) | 0.03017(9) |
| O1 | -0.0270(4) | 0.22488(14) | 0.0365(3) | 0.0400(5) |
| O2 | -0.0317(5) | 0.36506(18) | 0.0032(4) | 0.0513(6) |
| O3 | 0.1821(4) | 0.36348(15) | 0.7938(2) | 0.0485(5) |
| O4 | -0.0071(3) | 0.1205(2) | 0.31185(17) | 0.0394(4) |
| O5 | 0.3259(4) | 0.09026(18) | 0.2682(2) | 0.0596(8) |
| O1W | 0.0264(4) | 0.04024(15) | 0.0117(3) | 0.0378(5) |
| O2W | -0.3997(5) | 0.01936(18) | 0.1248(3) | 0.0399(6) |
| C1 | -0.1159(5) | 0.29758(18) | 0.0391(3) | 0.0362(6) |
| C2 | -0.3469(5) | 0.30396(18) | 0.0750(3) | 0.0372(6) |
| C3 | -0.3691(6) | 0.3822(2) | 0.1731(4) | 0.0436(7) |
| C4 | -0.2236(6) | 0.37633(19) | 0.3378(3) | 0.0400(6) |
| C5 | -0.3164(6) | 0.3471(3) | 0.4507(4) | 0.0503(8) |
| C6 | -0.1851(6) | 0.3411(2) | 0.6030(4) | 0.0495(8) |
| C7 | 0.0406(6) | 0.3665(2) | 0.6450(3) | 0.0384(7) |
| C8 | 0.1390(6) | 0.3952(2) | 0.5351(4) | 0.0521(8) |
| C9 | 0.0069(7) | 0.3999(3) | 0.3844(4) | 0.0502(9) |
| C10 | 0.2049(5) | 0.1087(3) | 0.3540(3) | 0.0390(8) |
| C11 | 0.3327(4) | 0.1152(3) | 0.5230(3) | 0.0346(5) |
| C12 | 0.2243(5) | 0.1360(3) | 0.6307(3) | 0.0435(9) |
| C13 | 0.3491(5) | 0.1377(2) | 0.7839(3) | 0.0439(9) |
| C14 | 0.6793(5) | 0.1044(3) | 0.7283(3) | 0.0545(12) |
| C15 | 0.5656(5) | 0.1008(3) | 0.5744(3) | 0.0546(12) |
| N1 | -0.4019(6) | 0.22134(18) | 0.1386(4) | 0.0358(7) |
| N2 | 0.5747(3) | 0.1215(3) | 0.8348(2) | 0.0366(4) |

**Table 4.3** Atomic coordinates and equivalent isotropic displacement parameters for **III**.

| | ***x*** | ***y*** | ***z*** | ***Ueq*** **(Å$^2$)** |
|---|---|---|---|---|
| Ni1 | 0.7941(2) | 0.12114(7) | 0.07252(12) | 0.0389(3) |
| O1 | 0.9839(15) | 0.2218(4) | 0.0344(11) | 0.049(2) |
| O2 | 0.980(2) | 0.3638(6) | -0.0010(13) | 0.060(2) |
| O3 | 1.1938(14) | 0.3628(5) | 0.7958(8) | 0.056(2) |
| O4 | 0.9972(10) | 0.1199(8) | 0.3087(6) | 0.0447(13) |
| O5 | 1.3362(13) | 0.0917(5) | 0.2675(8) | 0.066(3) |
| O1W | 1.0260(16) | 0.0398(5) | 0.0170(9) | 0.048(2) |
| O2W | 0.6023(16) | 0.0221(6) | 0.1203(11) | 0.047(2) |
| C1 | 0.894(2) | 0.2960(6) | 0.0379(10) | 0.046(3) |
| C2 | 0.666(2) | 0.3028(6) | 0.0711(11) | 0.046(2) |
| C3 | 0.646(2) | 0.3808(6) | 0.1671(12) | 0.050(3) |
| C4 | 0.789(2) | 0.3748(6) | 0.3352(11) | 0.047(3) |
| C5 | 0.695(2) | 0.3477(8) | 0.4462(13) | 0.060(3) |
| C6 | 0.828(2) | 0.3412(8) | 0.6016(12) | 0.058(3) |
| C7 | 1.056(2) | 0.3660(7) | 0.6427(14) | 0.049(3) |
| C8 | 1.154(3) | 0.3925(8) | 0.5376(15) | 0.064(3) |
| C9 | 1.015(3) | 0.3997(8) | 0.3799(15) | 0.061(4) |
| C10 | 1.2131(19) | 0.1090(9) | 0.3512(11) | 0.048(3) |
| C11 | 1.3396(17) | 0.1159(12) | 0.5243(10) | 0.048(2) |
| C12 | 1.2331(19) | 0.1308(11) | 0.6313(11) | 0.056(3) |
| C13 | 1.3611(19) | 0.1326(10) | 0.7865(12) | 0.058(3) |
| C14 | 1.6928(18) | 0.1104(12) | 0.7324(11) | 0.062(3) |
| C15 | 1.5794(18) | 0.1083(13) | 0.5752(12) | 0.069(4) |
| N1 | 0.613(2) | 0.2197(6) | 0.1364(13) | 0.045(3) |
| N2 | 1.5883(13) | 0.1224(10) | 0.8376(8) | 0.0469(17) |

**Table 4.4** Selected bond distances and angles in **II**.

| | | | |
|---|---|---|---|
| *Bond distances (Å)* | | | |
| Co1–O1 | 2.057(2) | C1–O2 | 1.252(4) |
| Co1–O2W | 2.073(3) | C7–O3 | 1.379(4) |
| Co1–O1W | 2.118(2) | N1–C2 | 1.487(4) |
| Co1–N1 | 2.121(3) | O4–C10 | 1.243(3) |
| Co1–O4 | 2.1727(16) | C10–O5 | 1.253(3) |
| Co1–N2$^{i}$ | 2.1792(19) | C13–N2 | 1.334(4) |
| O1–C1 | 1.255(4) | N2–C14 | 1.334(4) |
| *Bond angles (°)* | | | |
| O1–Co1–O2W | 176.10(12) | O1W–Co1–O4 | 91.45(9) |
| O1–Co1–O1W | 88.15(11) | N1–Co1–O4 | 85.33(12) |
| O2W–Co1–O1W | 94.17(10) | O1–Co1—N2$^{i}$ | 91.45(12) |
| O1–Co1–N1 | 80.50(12) | O2W–Co1–N2$^{i}$ | 91.72(12) |
| O2W–Co1–N1 | 97.00(8) | O1W–Co1–N2$^{i}$ | 89.27(10) |
| O1W–Co1–N1 | 168.24(11) | N1–Co1–N2$^{i}$ | 94.04(13) |
| O1–Co1–O4 | 88.98(11) | O4–Co1–N2$^{i}$ | 179.18(8) |
| O2W–Co1–O4 | 87.83(11) | | |

[a] Symmetry code: (i) $x$ - 1, $y$, $z$ - 1.

**Table 4.5** Selected bond distances and angles in **III**.

| | | | |
|---|---|---|---|
| *Bond distances (Å)* | | | |
| Ni1–O1 | 2.030(8) | C1–O2 | 1.271(14) |
| Ni1–O2W | 2.052(9) | N1–C2 | 1.493(14) |
| Ni1–O1W | 2.066(9) | C7–O3 | 1.394(15) |
| Ni1–N1 | 2.067(11) | O4–C10 | 1.264(12) |
| Ni1–N2$^{i}$ | 2.126(7) | C10–O5 | 1.252(12) |
| Ni1–O4 | 2.131(5) | C13–N2 | 1.329(13) |
| O1–C1 | 1.276(13) | N2–C14 | 1.316(12) |
| *Bond angles (°)* | | | |
| O1–Ni1–O2W | 177.4(4) | O1W–Ni1–N2$^{i}$ | 89.8(4) |
| O1–Ni1–O1W | 87.4(4) | N1–Ni1–N2$^{i}$ | 94.3(4) |
| O2W–Ni1–O1W | 94.3(4) | O1–Ni1–O4 | 89.7(4) |
| O1–Ni1–N1 | 82.3(5) | O2W–Ni1–O4 | 88.3(4) |
| O2W–Ni1–N1 | 95.8(3) | O1W–Ni1–O4 | 90.7(3) |
| O1W–Ni1–N1 | 169.0(4) | N1–Ni1–O4 | 85.3(4) |
| O1–Ni1–N2$^{i}$ | 90.7(4) | N2$^{i}$–Ni1–O4 | 179.4(3) |
| O2W–Ni1–N2$^{i}$ | 91.3(4) | | |

[a] Symmetry code: (i) $x$ - 1, $y$, $z$ - 1.

## 4.2 Results and discussion

### 4.2.1 Description of crystal structures

X-ray single crystal diffraction revealed that crystals **II** and **III** are isostructural. They crystallize in the same monoclinic crystal system with the non–centrosymmetric $P2_1$ space group. The asymmetric unit consists of a single metal ion; Co$^{II}$ for **II** and Ni$^{II}$ for **III**, one tyrosinate ion, one isonicotinate ion and two coordinated water molecules as shown in Fig. 4.1.

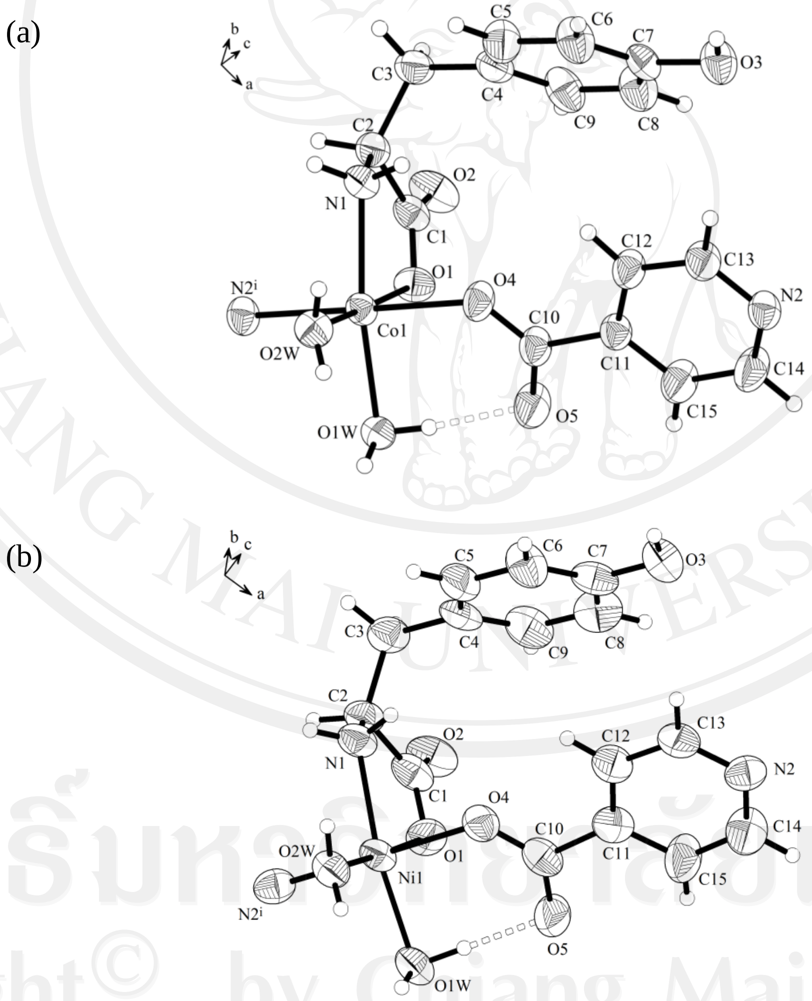

**Fig. 4.1** View of extended asymmetric units of (a) **II** and (b) **III** with 50% thermal ellipsoids and atomic labeling for non–hydrogen atoms. The hydrogen bond shows in dotted lines. Symmetry code: (i) $x$ - 1, $y$, $z$ - 1.

Subsequent structure discussion will only concentrate on compound **II** because of the similarity between **II** and **III**. $Co^{II}$ has an octahedral geometry and is coordinated by one deprotonated chelating tyrosine molecule through N and O atoms of amino acid group (Co1–N1 = 2.121(3) Å, Co1–O1 = 2.057(2) Å), one N atom of the pyridine ring (Co1–N2 = 2.172(19) Å) and one monodentate carboxylate group (Co1–O4 = 2.1727(16) Å) from isonicotinate, and two water molecules (Co1–O1W = 2.118(2) Å and Co1–O2W = 2.073(3) Å) . The isonicotinate ion act as bridging ligand, connecting pairs of $Co^{II}$ centers *via* Co–O and Co–N bonds to build a 1–D chain with composition $[Co(C_9H_{10}NO_3)(C_6H_4NO_2)(H_2O)_2]_n$ as shown in Fig. 4.2. The linear one–dimensional chain is formed from non–centrosymmetric coordination of $Co^{II}$ by isonicotinate and decorated by water molecules and tyrosinate. The result is chiral one–dimensional chains that run parallel to the crystallographic [1 0 1] direction.

**Fig. 4.2** Illustration of the one–dimensional coordination polymer $[Co(C_9H_{10}NO_3)(C_6H_4NO_2)(H_2O)_2]_n$ chain within **II**. Color scheme: Ni, black; O, dark grey; N, light grey; C, grey.

The three–dimensional architecture is produced by the stacking of these chains in an ABAB manner along the *b*–axis, as shown in Fig. 4.3a. Within the unit cell, two chains are related by the $2_1$ screw axis. Unit vector translations combined with the screw axis generate a checkerboard arrangement of chains that run along [1 0 1] direction (Fig. 4.3b).

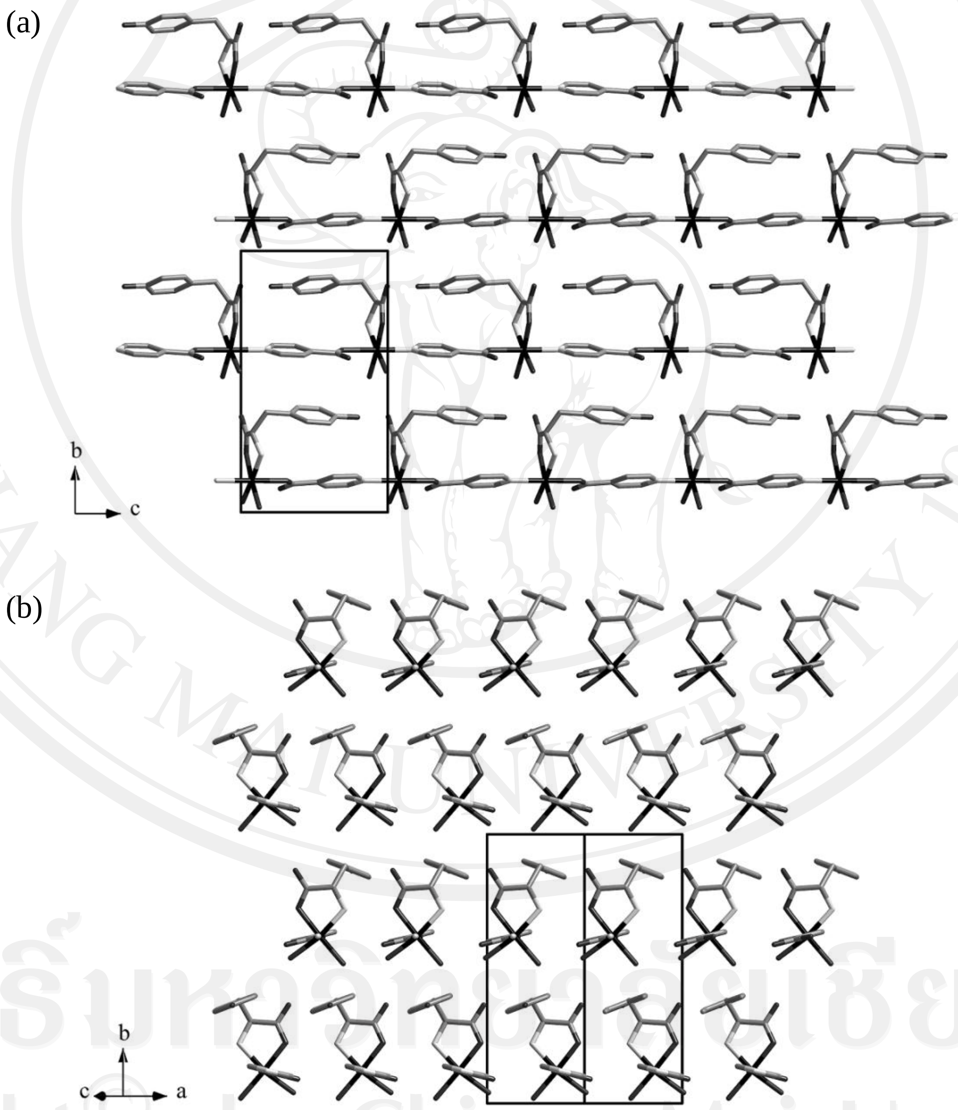

**Fig. 4.3** Views of (a) ABAB stacking of the $[Co(C_9H_{10}NO_3)(C_6H_4NO_2)(H_2O)_2]_n$ chains parallel to the *b*–axis and (b) checkerboard arrangement of the chains along [1 0 1] direction.

The structure is stabilized by the hydrogen bonding interactions as listed in Table 4.6. The intra−chain hydrogen bond is formed between the carboxylate group of isonicotinate and one of coordinated water molecule, O1W−H1D···O5, where the O···O distance is 2.626(3) Å. The chain stacking is stabilized by the inter−hydrogen bonding interactions with four different types. The first and second important hydrogen bonds are created by the coordinated water and both of carboxylate and hydroxyl groups of tyrosine, O1W−H1C···O2$^{\mathrm{i}}$ (Fig. 4.4a) and O2W−H2C···O3$^{\mathrm{ii}}$ (Fig. 4.4b), respectively. The third is formed by the carboxylate group of isonicotinic acid and water (O2W−H2D···O5$^{\mathrm{iii}}$) as illustrated in (Fig. 4.4c). The last inter−chain hydrogen bond is formed by the intermolecular tyrosine through hydroxyl and carboxylate groups, O3−H3···O2$^{\mathrm{iv}}$ (Fig. 4.4c). It is noteworthy that tyrosine is involved as a donor in the O3−H3···O2 hydrogen bond as well as an acceptor in the O1W−H1C···O2 and O2W−H2C···O3 hydrogen bonds. In addition, coordinated water molecules play an important role in the hydrogen bonding present. One molecule is involved both in intra− and inter−chain bonding and the other one participates only in the inter−chain bonding.

**Table 4.6** Details of the hydrogen bonding interactions in **II**. A hydrogen bond donor and acceptor atoms are denoted as D and A, respectively.

| D–H···A $^{a}$ | D–H, (Å) | H···A, (Å) | D···A, (Å) | ∠ D–H···A, (°) |
|---|---|---|---|---|
| O1W–H1C···O2$^{\mathrm{i}}$ | 0.87(2) | 1.89(3) | 2.726(4) | 160(4) |
| O1W–H1D···O5 | 0.86(2) | 1.77(2) | 2.626(3) | 174(4) |
| O2W–H2C···O3$^{\mathrm{ii}}$ | 0.84(2) | 1.91(2) | 2.754(4) | 177(4) |
| O2W–H2D···O5$^{\mathrm{iii}}$ | 0.84(2) | 1.83(2) | 2.642(3) | 160(3) |
| O3–H3···O2$^{\mathrm{iv}}$ | 0.82 | 1.82 | 2.607(3) | 161.44 |

$^{a}$ Symmetry codes: (i) $-x, y - ½, -z$; (ii) $-x, y - ½, -z + 1$; (iii) $x - 1, y, z$; (iv) $x, y, z + 1$.

The one–dimensional chains are linked together by hydrogen–bonded sheets perpendiculars to the chains. The result is a three–dimensional solid that has both coordination polymer and hydrogen–bonding sheet parts.

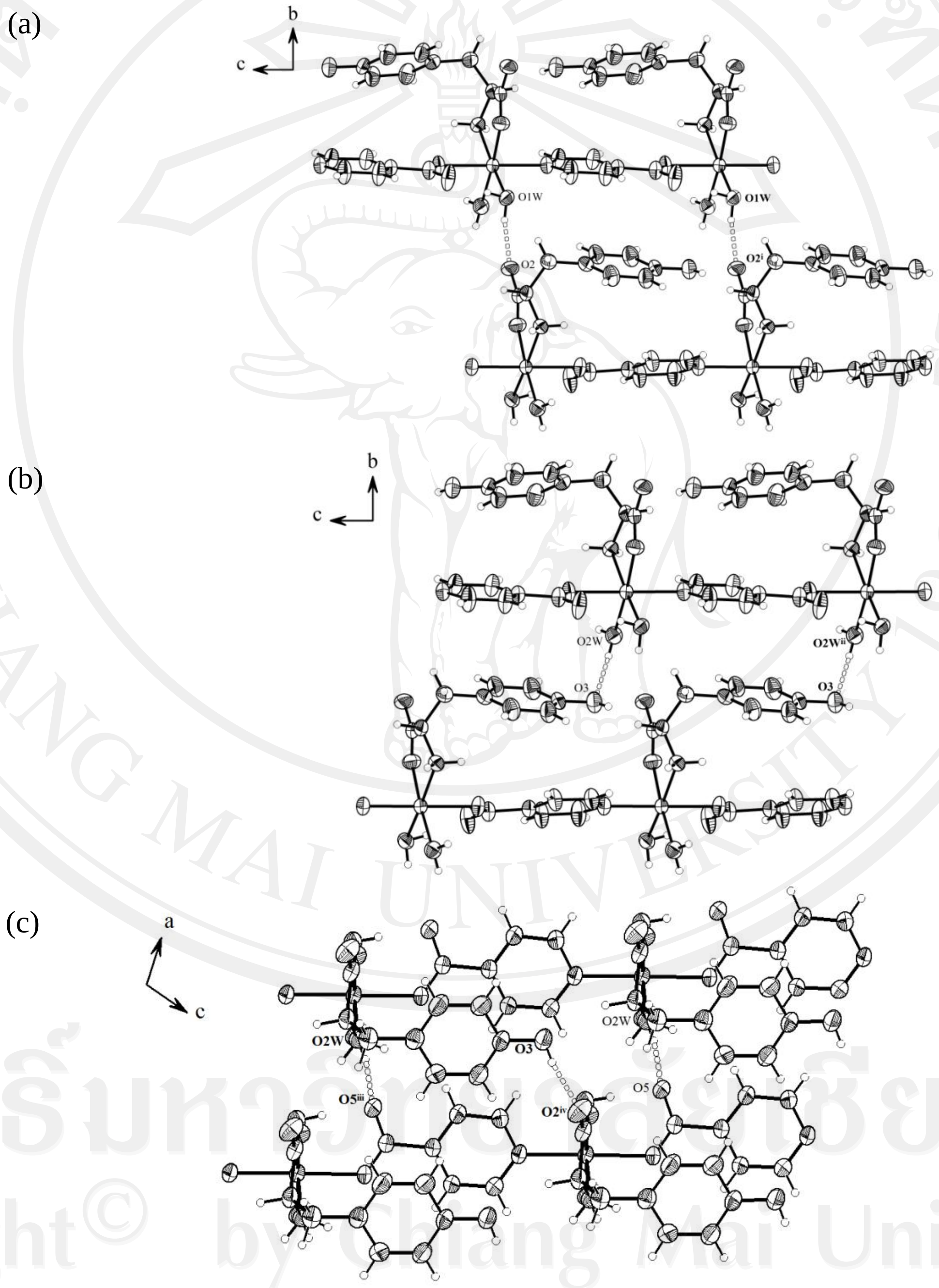

**Fig. 4.4** Representation of the hydrogen bonding interactions (dotted lines) in **II**, generated by (a) $-x, y-\frac{1}{2}, -z$, (b) $-x, y-\frac{1}{2}, -z+1$ and (c) $x-1, y, z$ and $x, y, z+1$.

### 4.2.2 The FT−IR spectra and thermal behaviors

The FT−IR spectra (Fig. 4.5) present the characteristic absorptions of the major functional groups of the crystal components. The broad band around 3400 cm$^{-1}$ can be assigned to the O−H stretching of water molecules. The characteristic medium strength band at 845 cm$^{-1}$ indicates the presence of coordinated water. The sharp and strong overlap band at 3330 cm$^{-1}$ and 1615 are assigned the N−H stretching and bending of the primary amino group of tyrosine, respectively. The asymmetric and the symmetric C=O stretching are observed at 1580 and 1400 cm$^{-1}$, respectively.

The thermogravimetric data for **II** and **III** are shown in Fig 4.6. These compounds each lose water upon heating but the stability of the two compounds is somewhat different. For **II** the trace is much less well defined with the first mass loss occurring in the range 40 to 260 °C, with mass loss 15.36%, rather greater than the loss of two coordinated water molecules (9.06%). There is a further broad mass loss above 300°C that may correspond to the loss of tyrosine (calc. 45.31%). For **III** a trace of mass *vs.* temperature upon heating displays a very well−defined first step with the loss of 10.05% (calc. 9.07%) around 300 °C. This corresponds to the loss of water molecules. The rather better defined decompositions for **III**, including a plateau between 280 °C and 370 °C, may be a reflection of the Ni$^{II}$ ion being more stable after the loss of two ligands than the Co$^{II}$. Experiments are underway to explore whether crystallinity is preserved in either sample upon thermal removal of water.

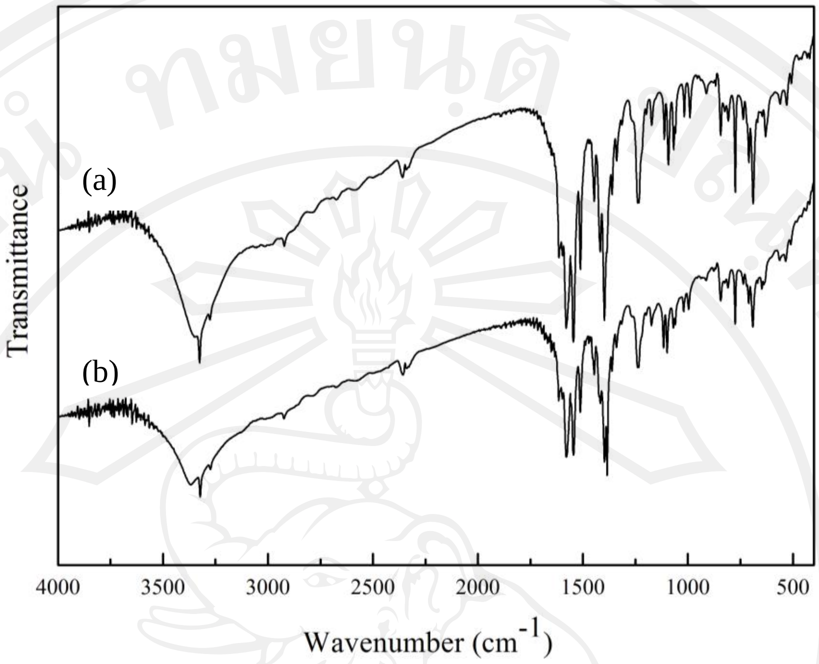

**Fig. 4.5** FT−IR spectra collected on the ground crystals of (a) **II** and (b) **III**.

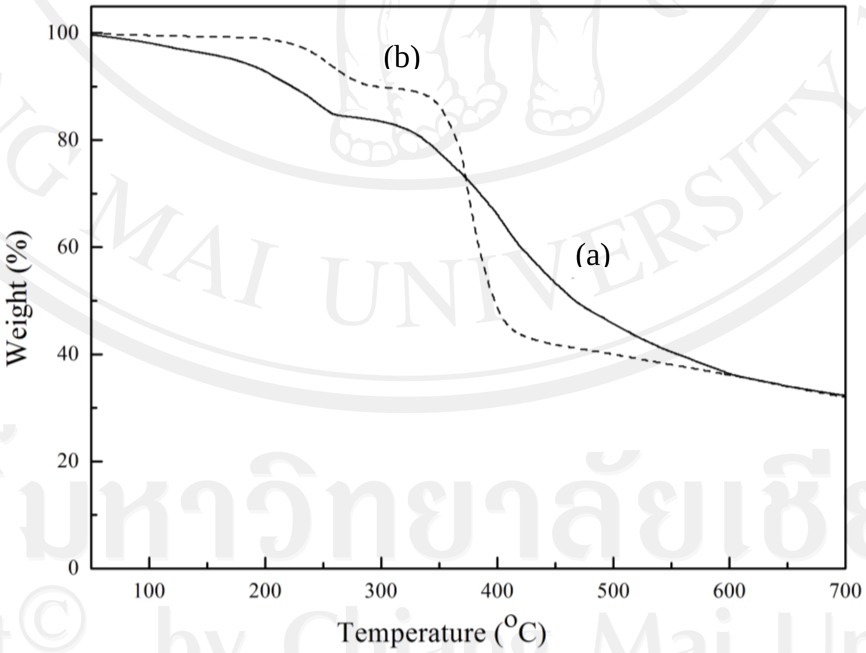

**Fig. 4.6** Thermogravimetric analysis of (a) **II** and (b) **III**.

## 4.3 Conclusions

The compounds described here demonstrate a little used strategy for the construction of chiral framework solids. The achiral linear chain present in **II** and **III** is decorated by a cheap, homochiral bidentate ligand. We are exploring this approach further in attempts to construct homochiral three-dimensional frameworks with appreciable porosity. The demonstration that tyrosine is a reliable chiral auxiliary ligand may prove important to this work. Modification of the reaction mixture to incorporate ligands known to form two and three dimensional frameworks is underway.

## REFERENCES

1. D. Bradshaw, J.B. Claridge, E.J. Cussen, T.J. Prior, M.J. Rosseinsky, Acc. Chem. Res. 38 (2005) 273.
2. J.M. Falkowski, S. Liu, W. Lin, Isr. J. Chem. 52 (2012) 603.
3. L. Ma, W. Lin, Top. Curr. Chem. 293 (2010) 175.
4. S. Qiu, G. Zhu, Coord. Chem. Rev. 253 (2009) 2891.
5. K. Gedrich, I. Senkovska, I.A. Baburin, U. Mueller, O. Trapp, S. Kaskel, Inorg. Chem. 49 (2010) 4440.
6. T. Hu, W. Bi, X. Hu, X. Zhao, D. Sun, Cryst. Growth. Des. 10 (2010) 3324.
7. A. Mantion, L. Massüger, P. Rabu, C. Palivan, L.B. McCusker, A. Taubert, J. Am. Chem. Soc. 130 (2008) 2517.
8. T.J. Prior, M.J. Rosseinsky, Inorg. Chem. 42 (2003) 1564.

9. D. Sun, Y. Ke, D.J. Collins, G.A. Lorigan, H.C. Zhou, Inorg. Chem. 46 (2007) 2725.
10. C.D. Wu, A. Hu, L. Zhang, W. Lin, J. Am. Chem. Soc. 127 (2005) 8940.
11. D. Zhao, D.J. Timmons, D. Yuan, H.C. Zhou, Acc. Chem. Res. 44 (2011) 123.
12. C.J. Kepert, T.J. Prior, M.J. Rosseinsky, J. Am. Chem. Soc. 122 (2000) 5158.
13. E. Farkas, I. Sóvágó, Amino Acids, Pept. Proteins 27 (2012) 66.
14. D.–Q. Li, J. Zhou, X. Liu, Acta. Crystallogr. C63 (2007) m371.
15. J. Weng, M. Hong, Q. Shi, R. Cao, A.S.C. Chan, Eur. J. Inorg. Chem. (2002) 2553.
16. H. Bußkamp, G.B. Deacon, M. Hilder, P.C. Junk, U.H. Kynast, W.W. Lee, D.R. Turner, Cryst. Eng. Comm. 9 (2007) 394.
17. C.N.R Rao, S. Natarajan, R. Vaidhyanathan, Angew. Chem. Int. Ed. 43 (2004) 1466.
18. O.M. Yaghi, M. O’Keeffe, N.W. Ockwig, H.K. Chae, M. Eddaoudi, J. Kim, Nature 423 (2003) 705.
19. G.M. Sheldrick, Acta. Cryst. A64 (2008) 112.